Journal of Science: Advanced Materials and Devices 1 (2016) 51–56

Contents lists available at ScienceDirect

Journal of Science: Advanced Materials and Devices

journal homepage: www.elsevier.com/locate/jsamd

Original article

Atomic and electronic structures of I-V-VI_2 ternary chalcogenides

Khang Hoang [a, *], Subhendra D. Mahanti [b]

[a] Center for Computationally Assisted Science and Technology, North Dakota State University, Fargo, ND, 58108, USA
[b] Department of Physics and Astronomy, Michigan State University, East Lansing, MI, 48824, USA

ARTICLE INFO

Article history:
Received 11 April 2016
Accepted 14 April 2016
Available online 22 April 2016

Keywords:
Ternary chalcogenide
I-V-VI2
Electronic structure
First-principles calculations

ABSTRACT

Atomic and electronic structures of I-V-VI_2 (I = Na, K, Ag, Cu, Au; V = As, Sb, Bi; VI = S, Se, Te) are studied using first-principles hybrid density functional calculations. We find that the strong hybridization between the trivalent cation (As, Sb, and Bi) *p* states and the divalent anion (S, Se, and Te) *p* states tends to introduce electronic states in the band gap or pseudogap region and drive the systems toward metallicity. The atomic ordering on the cation sublattice of the ternary chalcogenides, therefore, has a strong impact on the energetics and the electronic structure in the neighborhood of the Fermi level as it determines if a certain atomic configuration is favorable to the highly directional cation *p*–anion *p* interaction. Besides these *p* states, the *s* state (in the case of Na and K) or the *s* and *d* states (Ag, Cu, and Au) can also play an important role in the band-gap formation. Our study suggests how to manipulate the electronic structure of these ternary compounds such that they show desired features for different applications by modifying their atomic structure and/or by changing their constituent element(s).

1. Introduction

Ternary chalcogenides I-V-VI_2 have been studied in connection with thermoelectric, optical phase-change, and photovoltaic applications [1–3]. Among the Ag-Sb-based materials, $AgSbTe_2$, for example, is not only a good thermoelectric [1,4,5] but also the end-compound of a number of high-temperature high-performance thermoelectrics [6–8]. The material has a very low lattice thermal conductivity [1,4]. $AgSbTe_2$ was synthesized as early as in the late 1950s and long thought to have a rocksalt structure with random distribution of Ag and Sb ions on the face-centered cubic (*fcc*) cation sublattice [9,10]. Experimental evidence of the Ag/Sb ordering was confirmed only quite recently [11]. Other I-V-VI_2 compounds have also been synthesized and investigated [9,10,12,13], yet the atomic orderings on the lattice of many of these ternary compounds are still unknown or not well-defined.

On the theory side, we reported in 2007 first detailed studies of the atomic and electronic structures of I-V-VI_2 using first-principles density-functional theory (DFT) calculations [14,15]. Low-energy ordered structures of $AgSbTe_2$ and related compounds were discovered using a heuristic approach based on the interplay between the atomic and electronic structures [14]. These ordered structures were later confirmed by Barabash et al. [16] in their first-principles cluster expansion study and eventually supported by experimental observations [17,18]. Our early studies have also provided a good understanding of the atomic *vis-à-vis* electronic structures and the underlying physics of band-gap formation in the ternary chalcogenides. In nearly a decade since the 2007 works, there have been numerous first-principles investigations of the I-V-VI_2 compounds reported by different research groups [19–30]. Most of the studies to date, however, were carried out using standard DFT calculations within the local-density (LDA) or generalized-gradient (GGA) approximation that are known to often underestimate the band gap of semiconductors.

We herein revisit a series of I-V-VI_2 compounds (hereafter also denoted as ABQ_2; I = *A* = Na, K, Ag, Cu, Au; V = *B* = As, Sb, Bi; VI = *Q* = S, Se, Te) through extensive first-principles calculations using a hybrid DFT/Hartree-Fock approach. In order to conserve computing resources, we study these ternary chalcogenides mainly in the rhombohedral structure AF-II (space group $R\bar{3}m$), one of several possible ordered structures discussed in Refs. [14] and [15]; see also Fig. 1. Our study of the atomic and electronic structures begins with $AgSbQ_2$ and then continues with other ABQ_2 compounds. The focus is on changes in the electronic structure as one substitutes one constituent element in the compounds with another.

* Corresponding author.
E-mail address: khang.hoang@ndsu.edu (K. Hoang).
Peer review under responsibility of Vietnam National University, Hanoi.

http://dx.doi.org/10.1016/j.jsamd.2016.04.004

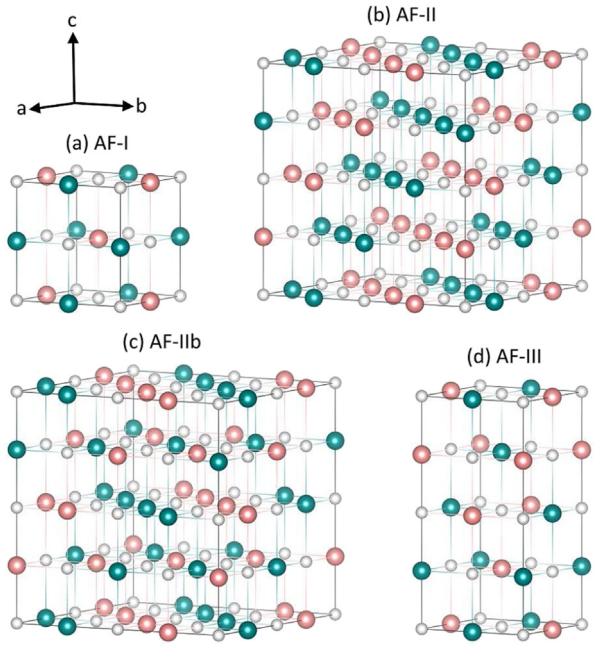

Fig. 1. Different structural models for $AgSbQ_2$ as described in Ref. [14]: (a) AF-I (space group: $P4/mmm$), (b) AF-II ($R\bar{3}m$), (c) AF-IIb ($F\bar{3}dm$), and (d) AF-III ($I4_1/amd$). Large spheres are for Ag and Sb, small spheres *Q*. The structures are named after the orderings of Ag and Sb ions, identified as up and down spins on the *fcc* cation sublattice [31,14], using the standard nomenclature of antiferromagnetic (AF) orderings [32].

2. Computational details

Our calculations for the structural and electronic properties of ABQ_2 compounds were based on DFT, using the Heyd-Scuseria-Ernzerhof (HSE06) screened hybrid functional [33,34], the projector augmented wave method [35,36], and a plane-wave basis set, as implemented in the Vienna *Ab Initio* Simulation Package (VASP) [37–39]. In these HSE06 calculations, we set the Hartree-Fock mixing parameter and the screening length to the standard values of 0.25 and 10 Å, respectively. The plane-wave basis-set cutoff was set to 300 eV, and a $5 \times 5 \times 5$ **k**-point mesh was used for the rhombohedral structure (4 atoms per primitive cell). Convergence with respect to self-consistent iterations was assumed when the total energy difference between cycles was less than 10^{-4} eV and the residual forces were less than 0.01 eV/Å. Scalar relativistic effects (mass-velocity and Darwin terms) and spin-orbit coupling (SOC) were included, except in the structural optimization where only the scalar relativistic effects were taken into account. The inclusion of SOC had been shown not to have significant influence on the structural properties [40].

3. Ag-Sb-based ternary chalcogenides

3.1. Atomic structure

It was initially reported, based on X-ray diffraction (XRD) measurements, that Ag and Sb were disordered on the cation sublattice of the NaCl-type structure of $AgSbQ_2$ [10]. Quarez et al. [11] in later XRD studies of single-crystal $AgSbTe_2$, however, showed evidence of Ag/Sb order in diffraction refinement using space groups $Pm\bar{3}m$, $P4/mmm$, and $R\bar{3}m$. On the theory side, we found a body-centered tetragonal structure with the space group $I4_1/amd$ in Monte Carlo simulations of $AgSbTe_2$ using a Coulomb lattice gas (ionic) model [31]. Other structures were also examined using DFT calculations, and low-energy ordered structures were searched for using a heuristic approach based on the interplay of the atomic and electronic structures [14]. Most significantly, we discovered a new ordered structure of $AgSbTe_2$, a cubic superstructure with the space group $F\bar{3}dm$ [denoted as AF-IIb; see Fig. 1 (c)], to be the lowest-energy structure [14]. AF-IIb is even lower in energy than the rhombohedral $R\bar{3}m$ structure [denoted as AF-II; see Fig. 1(b)] that had been used in the XRD refinement [11]; the total-energy difference is 74 meV per formula unit (f.u.) in HSE06 + SOC calculations. AF-II and AF-IIb, also known as trigonal "$L1_1$" and cubic "$D4$", respectively, in the literature, were later confirmed as the lowest-energy structures in a more comprehensive first-principles study by Barabash et al. [16] using a multicomponent cluster expansion approach. These two structures were also found to be compatible with observations from recent synchrotron X-ray diffuse scattering studies [18]. Results from the valence-band structure measurements carried out by Jovovic and Heremans [17] on high-quality crystals of $AgSbTe_2$ were consistent with the band structure calculated using the AF-IIb structure [14,15].

Fig. 1 shows four representative ordered structures of $AgSbQ_2$ as described in Ref. [14]; these are AF-I, AF-II, AF-IIb, and AF-III. The AF-II and AF-IIb structures were found to be degenerate in energy in the case of $AgSbSe_2$ and $AgSbS_2$, in DFT calculations within GGA parameterized by Perdew, Burke, and Ernzerhof (PBE) [42]. As discussed in detail in Ref. [14], the strong and directional interaction between the trivalent cation (Sb) *p* states and the divalent anion (S, Se, and Te) *p* states tends to introduce electronic states in the band gap region and drive the systems toward metallicity. The physical reason why AF-IIb (and AF-II) has a lower energy than all other structures is the presence of Ag in the Sb–*Q*–Sb … chains. It was found that the Ag in the chains strongly perturbs the hybridized Sb and *Q* *p*-bands, suppressing the electronic states coming from Sb and *Q* *p* states near the Fermi level or in the band gap region and resulting in a transfer of the electronic states to lower energies. The atomic ordering on the cation sublattice thus has a strong impact on the energetics of the ternaries and the electronic structure in the neighborhood of the Fermi level as it determines if a certain atomic configuration is favorable to the cation *p*–anion *p* interaction. It is noted that the highly directional cation *p*–anion *p* interaction has also been observed to play an important role in the energetics and the electronic structure of other narrow gap semiconductors such as thallium-based III-V-VI_2 ternary chalcogenides [43]. We summarize in Table 1 the structural properties of $AgSbQ_2$, focusing only on the simpler, rhombohedral AF-II structure. Our previous PBE results are also included for comparison. The calculated lattice constants of $AgSbTe_2$ are found to be in good agreement with the experimental values.

3.2. Electronic structure

Fig. 2 shows the total and projected density of states (DOS) of $AgSbTe_2$ in the AF-II structure. In the region near the Fermi level (at

Table 1
Lattice parameters of $AgSbQ_2$ (Q = Te, Se, S) in the rhombohedral AF-II structure, given in the hexagonal representation.

Compound		Lattice parameters (Å)	
$AgSbTe_2$	PBE	$a = 4.3842$, $c = 21.0118$	Ref. [14]
	HSE06	$a = 4.3446$, $c = 20.8042$	This work
	Expt.	$a = 4.2898(6)$, $c = 21.016(4)$	Ref. [11]
$AgSbSe_2$	PBE	$a = 4.1256$, $c = 19.9373$	Ref. [15]
	HSE06	$a = 4.0883$, $c = 19.7053$	This work
$AgSbS_2$	PBE	$a = 3.9641$, $c = 19.1091$	Ref. [15]
	HSE06	$a = 3.9359$, $c = 18.9360$	This work

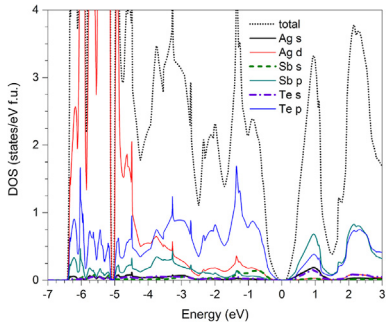

Fig. 2. Total and projected density of states (DOS) of rhombohedral $AgSbTe_2$ obtained in HSE06 calculations; f.u. = formula unit. The zero of energy is set to the highest occupied state.

0 eV), the top of the valence band is predominantly Te *p* states with some contributions from Ag *d* and Sb *s* states. The bottom of the conduction band is, on the other hand, predominantly Sb *p* states and some contributions from Ag *s* and Te *s* states. There is no real gap in the DOS but a pseudogap. The features in the electronic structure of $AgSbQ_2$ in the pseudogap region are shown more clearly in the band structure in Fig. 3.

The band structure of rhombohedral $AgSbTe_2$ indicates that the compound is a semimetal with an indirect band gap of about −0.3 eV calculated within HSE06 calculations, or can be regarded as a negative-gap semiconductor; see Fig. 3. The top of the valence band is Te *p*–Sb *p* derived, and the valence-band maximum (VBM) locates in the Γ–*X* line. The conduction-band minimum (CBM) locates near the *B* point and along the *B*–Γ line with the dispersive conduction band coming across the Fermi level. This band and a similar band at the *L* point can be, for simplicity, referred to as the "Ag *s* band" as discussed in Ref. [14]; they are derived from the Ag *s* state that strongly hybridizes with the Sb *p* states, as can also be seen in Fig. 2 in the energy range from 0 to 1.5 eV.

In going from $AgSbTe_2$ to $AgSbSe_2$ and $AgSbS_2$, the relative separation between the "Ag *s* bands" at the *L* point and near the *B* point and the valence band increases and the latter two compounds become semiconductors with indirect band gaps of 0.21 and 0.57 eV within HSE06, respectively; see Fig. 3. For comparison, the band gap values were found to be about 0 and 0.1 eV for the selenide and sulfide, respectively, within PBE calculations [15]. The CBM of rhombohedral $AgSbSe_2$ and $AgSbS_2$ is now at the *Z* point where the conduction-band extremum is Sb *p*–Te *p* derived. The separation between the conduction-band bottom (predominantly

Table 2
Lattice parameters of several ABQ_2 compounds (A = Na, K, Ag, Au; B = As, Sb, Bi; Q = Te, Se) in the rhombohedral AF-II structure, given in the hexagonal representation.

Compound		Lattice parameters (Å)	
$NaSbTe_2$	PBE	$a = 4.3896$, $c = 22.4228$	Ref. [15]
	HSE06	$a = 4.3848$, $c = 22.4812$	This work
$KSbTe_2$	PBE	$a = 4.4250$, $c = 24.6304$	Ref. [15]
	HSE06	$a = 4.4728$, $c = 24.8879$	This work
$CuSbTe_2$	HSE06	$a = 4.2165$, $c = 20.0882$	This work
$AuSbTe_2$	HSE06	$a = 4.3012$, $c = 20.2161$	This work
$AgAsTe_2$	PBE	$a = 4.1955$, $c = 20.4147$	Ref. [15]
	HSE06	$a = 4.1590$, $c = 20.5632$	This work
$AgBiTe_2$	PBE	$a = 4.4654$, $c = 21.3798$	Ref. [15]
	HSE06	$a = 4.4063$, $c = 21.0505$	This work
	Expt.	$a = 4.37(2)$, $c = 20.76(5)$	Ref. [10]
$AgBiSe_2$	HSE06	$a = 4.1649$, $c = 19.8209$	This work
	Expt.	$A = 4.184$, $c = 19.87$	Ref. [47]

Sb *p* states) and the valence-band top (predominantly chalcogen *p* states) increases in going from Te and Se to S, which is consistent with the trend in the relative positions between the *p* levels of Sb and the chalcogens in the Harrison's *Solid-State Table* [44].

4. Other I-V-VI_2 ternary chalcogenides

4.1. Atomic structure

$NaSbSe_2$, $NaSbTe_2$, and $NaBiTe_2$ were reported to have the NaCl-type structure with the lattice constant $a = 5.966(2)$, 6.317(2), and 6.366(3) Å, respectively; $NaAsSe_2$, on the other hand, crystallized in an orthorhombic (*Pbca*) structure with $a = 5.83 \pm 0.01$, $b = 24.27 \pm 0.05$, and $c = 11.82 \pm 0.02$ Å [12]. To our knowledge, there has been no reported information about $KSbTe_2$, although the structural properties of the other K-based ternary chalcogenides are available in the literature; e.g., $KAsSe_2$ crystallizes in a monoclinic (*Cc*) structure [45] and $KSbSe_2$ can be described by the space group *C*2/*m* [46]. Information about the atomic ordering on the cation sublattice in these compounds is still lacking. As regards $AgBiQ_2$, the compounds were reported to possess a statistically disordered NaCl-type structure at high temperatures and a rhombohedral structure at room temperature [10].

Among the structural models AF-I, AF-II, AF-IIb, and AF-III as presented in Fig. 1, $NaSbTe_2$ and $KSbTe_2$ were found to have the lowest energy in the AF-II structure; whereas in $AgAsTe_2$ and $AgBiTe_2$ AF-II and AF-IIb were found to be almost degenerate in energy in PBE calculations [15]. There appears to be a tendency for the $ASbTe_2$ compounds to adopt the rhombohedral structure when one replaces

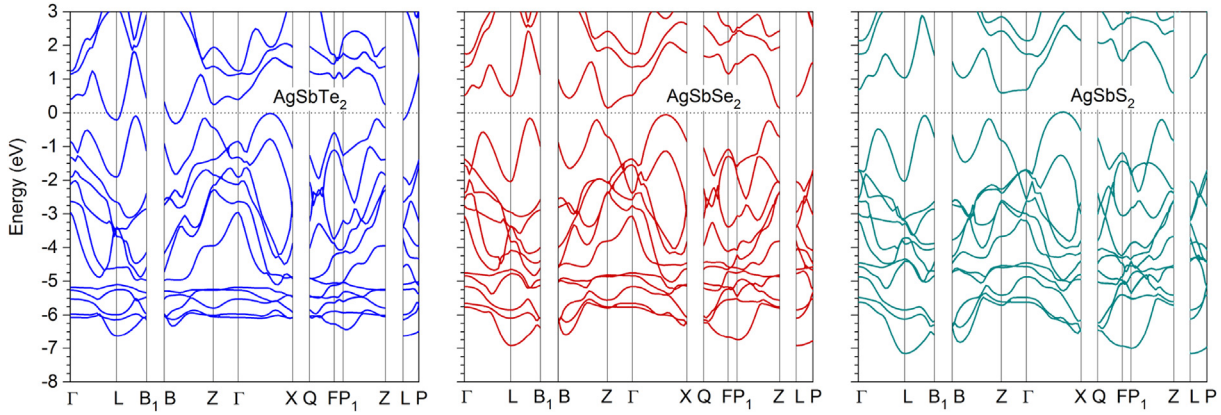

Fig. 3. Band structures of $AgSbTe_2$, $AgSbSe_2$, and $AgSbS_2$ in the rhombohedral AF-II structure. The symmetry lines in the rhombohedral Brillouin zone are chosen following Ref. [41].

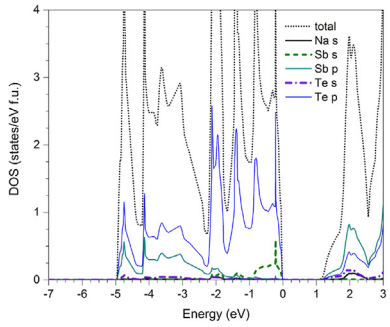

Fig. 4. Total and projected DOS of rhombohedral $NaSbTe_2$. The zero of energy is set to the highest occupied state.

A = Ag with a more ionic element (such as Na and K). It should be noted that the search for low-energy structures of these ABQ_2 compounds in Ref. [15] was not exhaustive. Indeed, we find that the hexagonal ($P\bar{3}m1$) structure [48] is lower in energy than the AF-II structure in $AgBiQ_2$; the energy difference is 70 meV/f.u. (Q = Te) or 49 meV/f.u. (Se) in HSE06 + SOC calculations. In Table 2, we list the lattice parameters of a number of ABQ_2 compounds only in the AF-II structure; the lattice parameters for rhombohedral $AgBiQ_2$ are in good agreement with the experimental values. We will look further into these compounds and see how the electronic structure changes when one replaces one constituent element with another while keeping the atomic structure fixed at a certain ordering type (e.g., AF-II). In the previous section, we have analyzed the changes as one varies Q in the $AgSbQ_2$ series; we now keep Q fixed at Q = Te and vary either A (Ag → Na, K, Cu, Au) or B (Sb → As, Bi) in ABQ_2.

4.2. Electronic structure

Fig. 4 shows the total and projected DOS of $NaSbTe_2$ in the AF-II structure. The top of the valence-band is predominantly Te p states; there is also some contribution from the Sb s. The bottom of the conduction band, on the other hand, consists of Sb p and some contributions from Te s and Na s states. As discussed in detail in Ref. [15], there are significant changes in the electronic structure of $NaSbTe_2$ in going from the AF-I and AF-III structures to the AF-II and AF-IIb structures; the interruption of Sb–Te chains (present in AF-I and AF-III) by Na (in AF-II and AF-IIb) cleans up completely the electronic states just above the Fermi level and opens a rather large gap. The calculated band structure of $NaSbTe_2$ is shown in Fig. 5; the HSE06 band gap is 0.96 eV and indirect. Because the energy level of Na s is higher than that of Ag s [44], the CBM is no longer along the B–Z line like in $AgSbTe_2$ but at Z. The VBM is, on the other hand, now near the Z point. The electronic structure of $KSbTe_2$ is very similar to that of $NaSbTe_2$ as seen in Fig. 5; the compound has an indirect gap of 1.00 eV within HSE06.

One can also replace Ag in $AgSbTe_2$ with Cu to manipulate the top of the valence band through the Cu 3d states. The electronic structure of $CuSbTe_2$ in the as-yet hypothetical AF-II structure resembles that of rhombohedral $AgSbTe_2$, see Fig. 5. However, the calculated band gap is more negative due to the increased DOS in the pseudogap region. The difference is due to the Cu 4s level being lower in energy compared to Ag 5s and the Cu 3d states being higher in energy than the Ag 4d states. Experimentally, $CuSbTe_2$ was reported to possess a Bi_2Te_3-like hexagonal structure with a = 4.22 Å and c = 29.9 Å (at 300 K) [49]. We also examined $AuSbTe_2$ in the hypothetical AF-II structure and find that the pseudogap feature is much less pronounced than in $CuSbTe_2$ as the Au 5d states are more extended toward the conduction band than the Cu 3d states which pushes the chalcogen p states upwards and enhances the DOS near the Fermi level. This material is a metal and thus not likely to be a good thermoelectric.

Next we keep the monovalent and divalent atoms fixed and vary the trivalent atom, i.e., considering $AgBTe_2$ as B goes from As to Sb and Bi. Fig. 6 shows the calculated band structures of $AgAsTe_2$ and $AgBiTe_2$ in the AF-II structure. Rhombohedral $AgAsTe_2$ has a negative band gap of −0.43 eV within HSE06. In going from As to Bi, the pseudogap gets deeper and a gap of 0.29 eV opens up in rhombohedral $AgBiTe_2$, as seen in Fig. 6.

Finally, we also investigated the electronic structure of rhombohedral $AgBiSe_2$; the result is shown in Fig. 6. Compared to $AgBiTe_2$, in addition the larger separation between the valence-band top (predominantly Se p states) and the conduction-band bottom (predominantly Bi p states), the "Ag s bands" at the L point and near the B point are higher and the CBM changes from the Γ point (in the telluride) to very close to the Z point (in the selenide). The calculated band gap is 0.52 eV within HSE06. For comparison, the spectroscopically measured band gap was reported to be about 0.6 eV for pristine $AgBiSe_2$ [50].

5. Summary

We have discussed the atomic and electronic structures of I-V-VI_2 ternary chalcogenides obtained in HSE06 hybrid functional calculations. We find that, in addition to the p states of the trivalent cations (As, Sb, Bi) and divalent anions (S, Se, Te), the s state (in the case of Na and K) or the s and d states (Ag, Cu, and Au) also play an

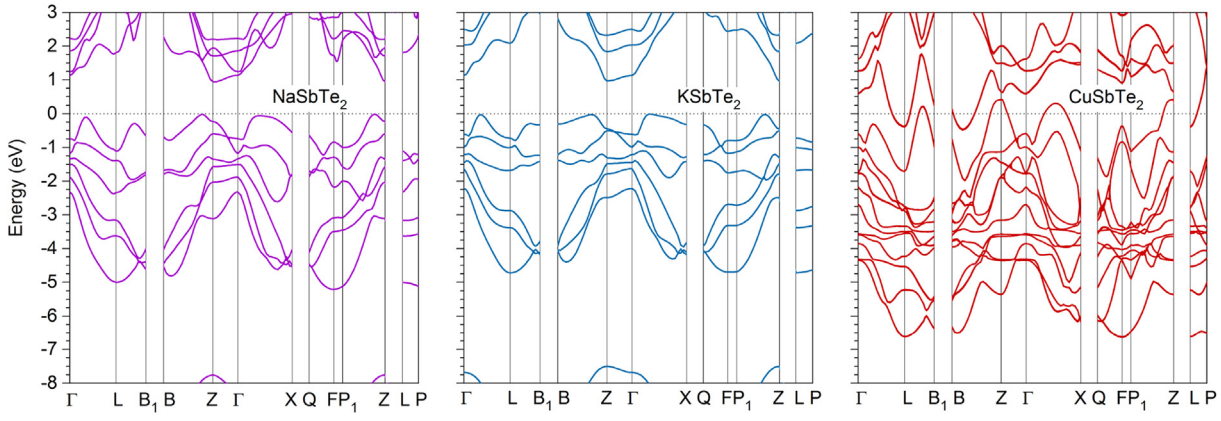

Fig. 5. Band structures of $NaSbTe_2$, $KSbTe_2$, and $CuSbTe_2$ in the rhombohedral AF-II structure.

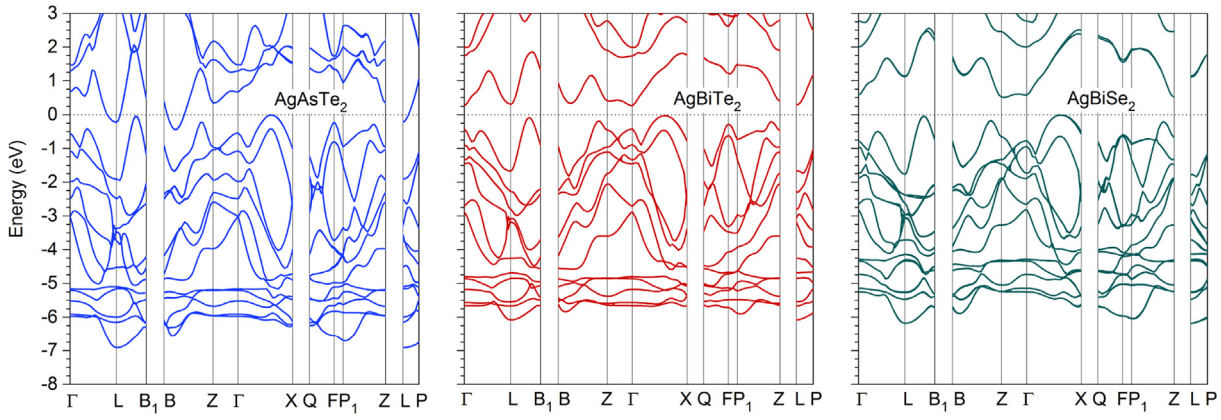

Fig. 6. Band structures of $AgAsTe_2$, $AgBiTe_2$, and $AgBiSe_2$ in the rhombohedral AF-II structure.

important role in the band-gap formation. These states impact the electronic structure near the band gap or pseudogap region through strong hybridization with the *p* states of the trivalent cations and divalent anions. The *s* state affects the electronic structure near the conduction-band bottom, whereas the *d* states affect the electronic structure near the valence-band top. Our study suggests how to manipulate the electronic structure of I-V-VI_2 ternaries such that they show desired features for different applications by modifying their atomic structure and/or by changing their constituent element(s). The results obtained in these calculations can provide experimentalists with guidance as they search for materials with certain properties and also to look at some of the promising materials more carefully. Finally, we find that hybrid functional calculations provide an improved description of the electronic structure of I-V-VI_2 compounds, especially the band gap value, over standard DFT calculations within GGA.

Acknowledgments

Work at North Dakota State University (NDSU) was supported by the U.S. Department of Energy Grant No. DE-SC0001717 and by NDSU's Center for Computationally Assisted Science and Technology.

References

[1] C. Wood, Materials for thermoelectric energy conversion, Rep. Prog. Phys. 51 (1988) 459, http://dx.doi.org/10.1088/0034-4885/51/4/001.
[2] R. Detemple, D. Wamwangi, M. Wuttig, G. Bihlmayer, Identification of Te alloys with suitable phase change characteristics, Appl. Phys. Lett. 83 (2003) 2572–2574, http://dx.doi.org/10.1063/1.1608482.
[3] L. Yu, R.S. Kokenyesi, D.A. Keszler, A. Zunger, Inverse design of high absorption thin-film photovoltaic materials, Adv. Energy Mater. 3 (2013) 43–48, http://dx.doi.org/10.1002/aenm.201200538.
[4] D.T. Morelli, V. Jovovic, J.P. Heremans, Intrinsically minimal thermal conductivity in cubic I-V-VI_2 semiconductors, Phys. Rev. Lett. 101 (2008) 035901, http://dx.doi.org/10.1103/PhysRevLett.101.035901.
[5] J. Xu, H. Li, B. Du, X. Tang, Q. Zhang, C. Uher, High thermoelectric figure of merit and nanostructuring in bulk $AgSbTe_2$, J. Mater. Chem. 20 (2010) 6138–6143, http://dx.doi.org/10.1039/C0JM00138D.
[6] K.F. Hsu, S. Loo, F. Guo, W. Chen, J.S. Dyck, C. Uher, T. Hogan, E.K. Polychroniadis, M.G. Kanatzidis, Cubic $AgPbmSbTe_{2+m}$: bulk thermoelectric materials with high figure of merit, Science 303 (2004) 818–821, http://dx.doi.org/10.1126/science.1092963.
[7] J. Androulakis, K.F. Hsu, R. Pcionek, H. Kong, C. Uher, J.J. D'Angelo, A. Downey, T. Hogan, M.G. Kanatzidis, Nanostructuring and high thermoelectric efficiency in p-type $Ag(Pb_{1-y}Sn_y)_mSbTe_{2+m}$, Adv. Mater. 18 (2006) 1170–1173, http://dx.doi.org/10.1002/adma.200502770.
[8] J. Androulakis, R. Pcionek, E. Quarez, J.-H. Do, H. Kong, O. Palchik, C. Uher, J.J. D'Angelo, J. Short, T. Hogan, M.G. Kanatzidis, Coexistence of large thermopower and degenerate doping in the nanostructured material $Ag_{0.85}SnSb_{1.15}Te_3$, Chem. Mater. 18 (2006) 4719–4721, http://dx.doi.org/10.1021/cm061151p.
[9] J. Wernick, K. Benson, New semiconducting ternary compounds, J. Phys. Chem. Solids 3 (1957) 157–159, http://dx.doi.org/10.1016/0022-3697(57)90066-5.
[10] S. Geller, J.H. Wernick, Ternary semiconducting compounds with sodium chloride-like structure: $AgSbSe_2$, $AgSbTe_2$, $AgBiS_2$, $AgBiSe_2$, Acta Crystallogr. 12 (1959) 46–54, http://dx.doi.org/10.1107/S0365110X59000135.
[11] E. Quarez, K.-F. Hsu, R. Pcionek, N. Frangis, E.K. Polychroniadis, M.G. Kanatzidis, Nanostructuring, compositional fluctuations, and atomic ordering in the thermoelectric materials $AgPbmSbTe_{2+m}$. The myth of solid solutions, J. Am. Chem. Soc. 127 (2005) 9177–9190, http://dx.doi.org/10.1021/ja051653o.
[12] B. Eisenmann, H. Schafer, Uber seleno- und telluroarsenite, -antimonite und -bismutite, Z. Anorg. Allg. Chem. 456 (1979) 87–94, http://dx.doi.org/10.1002/zaac.19794560109.
[13] A.P. Deshpande, V.B. Sapre, C. Mande, X-ray spectroscopic study of some ternary compounds of the type $A^IB^{III}C_2^{VI}$ and $A^IB^VCC_2^{VI}$, J. Phys. C Solid State Phys. 17 (1984) 955, http://dx.doi.org/10.1088/0022-3719/17/5/022.
[14] K. Hoang, S.D. Mahanti, J.R. Salvador, M.G. Kanatzidis, Atomic ordering and gap formation in Ag-Sb-based ternary chalcogenides, Phys. Rev. Lett. 99 (2007) 156403, http://dx.doi.org/10.1103/PhysRevLett.99.156403.
[15] K. Hoang, Atomic and Electronic Structures of Novel Ternary and Quaternary Narrow Band-Gap Semiconductors, Ph.D. thesis, Michigan State University, 2007.
[16] S.V. Barabash, V. Ozolins, C. Wolverton, First-principles theory of competing order types, phase separation, and phonon spectra in thermoelectric $AgPb_mSbTe_{m+2}$ alloys, Phys. Rev. Lett. 101 (2008) 155704, http://dx.doi.org/10.1103/PhysRevLett.101.155704.
[17] V. Jovovic, J.P. Heremans, Measurements of the energy band gap and valence band structure of $AgSbTe_2$, Phys. Rev. B 77 (2008) 245204, http://dx.doi.org/10.1103/PhysRevB.77.245204.
[18] J. Ma, O. Delaire, E.D. Specht, A.F. May, O. Gourdon, J.D. Budai, M.A. McGuire, T. Hong, D.L. Abernathy, G. Ehlers, E. Karapetrova, Phonon scattering rates and atomic ordering in $Ag_{1-x}Sb_{1+x}Te_{2+x}$ ($x = 0, 0.1, 0.2$) investigated with inelastic neutron scattering and synchrotron diffraction, Phys. Rev. B 90 (2014) 134303, http://dx.doi.org/10.1103/PhysRevB.90.134303.
[19] L.-H. Ye, K. Hoang, A.J. Freeman, S.D. Mahanti, J. He, T.M. Tritt, M.G. Kanatzidis, First-principles study of the electronic, optical, and lattice vibrational properties of $AgSbTe_2$, Phys. Rev. B 77 (2008) 245203, http://dx.doi.org/10.1103/PhysRevB.77.245203.
[20] K. Wojciechowski, M. Schmidt, J. Tobola, M. Koza, A. Olech, R. Zybała, Influence of doping on structural and thermoelectric properties of $AgSbSe_2$, J. Electron. Mater. 39 (2009) 2053–2058, http://dx.doi.org/10.1007/s11664-009-1008-8.
[21] S.V. Barabash, V. Ozolins, Order, miscibility, and electronic structure of Ag(Bi,Sb)Te_2 alloys and (Ag,Bi,Sb)Te precipitates in rocksalt matrix: a first-principles study, Phys. Rev. B 81 (2010) 075212, http://dx.doi.org/10.1103/PhysRevB.81.075212.
[22] J.T.R. Dufton, A. Walsh, P.M. Panchmatia, L.M. Peter, D. Colombara, M.S. Islam, Structural and electronic properties of $CuSbS_2$ and $CuBiS_2$: potential absorber materials for thin-film solar cells, Phys. Chem. Chem. Phys. 14 (2012) 7229–7233, http://dx.doi.org/10.1039/C2CP40916J.
[23] C. Xiao, X. Qin, J. Zhang, R. An, J. Xu, K. Li, B. Cao, J. Yang, B. Ye, Y. Xie, High thermoelectric and reversible p-n-p conduction type switching integrated in dimetal chalcogenide, J. Am. Chem. Soc. 134 (2012) 18460–18466, http://dx.doi.org/10.1021/ja308936b.
[24] M.D. Nielsen, V. Ozolins, J.P. Heremans, Lone pair electrons minimize lattice thermal conductivity, Energy Environ. Sci. 6 (2013) 570–578, http://dx.doi.org/10.1039/C2EE23391F.
[25] S. Berri, D. Maouche, N. Bouarissa, Y. Medkour, First principles study of structural, electronic and optical properties of $AgSbS_2$, Mat. Sci. Semicond. Process 16 (2013) 1439–1446, http://dx.doi.org/10.1016/j.mssp.2013.04.009.

[26] N. Rezaei, S.J. Hashemifar, H. Akbarzadeh, Thermoelectric properties of $AgSbTe_2$ from first-principles calculations, J. Appl. Phys. 116 (2014) 103705, http://dx.doi.org/10.1063/1.4895062.
[27] Y. Zhang, V. Ozolins, D. Morelli, C. Wolverton, Prediction of new stable compounds and promising thermoelectrics in the Cu–Sb–Se system, Chem. Mater. 26 (2014) 3427–3435, http://dx.doi.org/10.1021/cm5006828.
[28] B. Yang, L. Wang, J. Han, Y. Zhou, H. Song, S. Chen, J. Zhong, L. Lv, D. Niu, J. Tang, $CuSbS_2$ as a promising earth-abundant photovoltaic absorber material: a combined theoretical and experimental study, Chem. Mater. 26 (2014) 3135–3143, http://dx.doi.org/10.1021/cm500516v.
[29] D.S. Parker, A.F. May, D.J. Singh, Benefits of carrier-pocket anisotropy to thermoelectric performance: the case of p-type $AgBiSe_2$, Phys. Rev. Appl. 3 (2015) 064003, http://dx.doi.org/10.1103/PhysRevApplied.3.064003.
[30] H. Shinya, A. Masago, T. Fukushima, H. Katayama-Yoshida, Inherent instability by antibonding coupling in $AgSbTe_2$, Jpn. J. Appl. Phys. 55 (2016) 041801, http://dx.doi.org/10.7567/JJAP.55.041801.
[31] K. Hoang, K. Desai, S.D. Mahanti, Charge ordering and self-assembled nanostructures in a fcc Coulomb lattice gas, Phys. Rev. B 72 (2005) 064102, http://dx.doi.org/10.1103/PhysRevB.72.064102.
[32] M.K. Phani, J.L. Lebowitz, M.H. Kalos, Monte Carlo studies of an fcc Ising antiferromagnet with nearest- and next-nearest-neighbor interactions, Phys. Rev. B 21 (1980) 4027–4037, http://dx.doi.org/10.1103/PhysRevB.21.4027.
[33] J. Heyd, G.E. Scuseria, M. Ernzerhof, Hybrid functionals based on a screened coulomb potential, J. Chem. Phys. 118 (2003) 8207–8215, http://dx.doi.org/10.1063/1.1564060.
[34] J. Paier, M. Marsman, K. Hummer, G. Kresse, I.C. Gerber, J.G. Ángyán, Screened hybrid density functionals applied to solids, J. Chem. Phys. 124 (2006) 154709, http://dx.doi.org/10.1063/1.2187006.
[35] P.E. Blöchl, Projector augmented-wave method, Phys. Rev. B 50 (1994) 17953–17979, http://dx.doi.org/10.1103/PhysRevB.50.17953.
[36] G. Kresse, D. Joubert, From ultrasoft pseudopotentials to the projector augmented-wave method, Phys. Rev. B 59 (1999) 1758–1775, http://dx.doi.org/10.1103/PhysRevB.59.1758.
[37] G. Kresse, J. Hafner, Ab initio molecular dynamics for liquid metals, Phys. Rev. B 47 (1993) 558–561, http://dx.doi.org/10.1103/PhysRevB.47.558.
[38] G. Kresse, J. Furthmüller, Efficient iterative schemes for ab initio total-energy calculations using a plane-wave basis set, Phys. Rev. B 54 (1996) 11169–11186, http://dx.doi.org/10.1103/PhysRevB.54.11169.
[39] G. Kresse, J. Furthmüller, Efficiency of ab-initio total energy calculations for metals and semiconductors using a plane-wave basis set, Comput. Mater. Sci. 6 (1996) 15–50, http://dx.doi.org/10.1016/0927-0256(96)00008-0.
[40] L.E. Ramos, L.K. Teles, L.M.R. Scolfaro, J.L.P. Castineira, A.L. Rosa, J.R. Leite, Structural, electronic, and effective-mass properties of silicon and zinc-blende group-III nitride semiconductor compounds, Phys. Rev. B 63 (2001) 165210, http://dx.doi.org/10.1103/PhysRevB.63.165210.
[41] W. Setyawan, S. Curtarolo, High-throughput electronic band structure calculations: challenges and tools, Comput. Mater. Sci. 49 (2010) 299–312, http://dx.doi.org/10.1016/j.commatsci.2010.05.010.
[42] J.P. Perdew, K. Burke, M. Ernzerhof, Generalized gradient approximation made simple, Phys. Rev. Lett. 77 (1996) 3865–3868, http://dx.doi.org/10.1103/PhysRevLett.77.3865.
[43] K. Hoang, S.D. Mahanti, Atomic and electronic structures of thallium-based III-V-VI_2 ternary chalcogenides: Ab initio calculations, Phys. Rev. B 77 (2008) 205107, http://dx.doi.org/10.1103/PhysRevB.77.205107.
[44] W.A. Harrison, "The Solid-state Table" in Elementary Electronic Structure, World Scientific, Singapore, 2004.
[45] M. Kapon, G.M. Reisner, R.E. Marsh, On the structure of $KAsSe_2$, Acta Crystallogr. Sec. C 45 (1989) 2029, http://dx.doi.org/10.1107/S010827018900870X.
[46] L.D. Calvert, Changes in published type structures, Acta Crystallogr. Sec. B 48 (1992) 113–114, http://dx.doi.org/10.1107/S0108768191009242.
[47] L. Pan, D. Brardan, N. Dragoe, High thermoelectric properties of n-type $AgBiSe_2$, J. Am. Chem. Soc. 135 (2013) 4914–4917, http://dx.doi.org/10.1021/ja312474n.
[48] P. Bayliss, Crystal chemistry and crystallography of some minerals in the tetradymite group, Am. Mineral. 76 (1991) 257–265.
[49] V.P. Zhuse, V.M. Sergeeva, E.L. Shtrum, Semiconducting compounds with a general formual ABX_2, Sov. Phys. Tech. Phys. 3 (1958) 1925–1938.
[50] S.N. Guin, V. Srihari, K. Biswas, Promising thermoelectric performance in n-type $AgBiSe_2$: effect of aliovalent anion doping, J. Mater. Chem. A 3 (2015) 648–655, http://dx.doi.org/10.1039/C4TA04912H.